222 J. Med. Chem. 2011, 54, 222–232
DOI: 10.1021/jm1011462

Journal of Medicinal Chemistry Article

Novel Antiviral C5-Substituted Pyrimidine Acyclic Nucleoside Phosphonates Selected as Human Thymidylate Kinase Substrates

Dimitri Topalis,[†,∞] Ugo Pradère,[‡,∞] Vincent Roy,[‡] Christophe Caillat,[§] Ahmed Azzouzi,[‡] Julie Broggi,[‡] Robert Snoeck,[∥] Graciela Andrei,[∥] Jay Lin,[⊥] Staffan Eriksson,[⊥] Julie A. C. Alexandre,[†] Chahrazade El-Amri,[†] Dominique Deville-Bonne,[†] Philippe Meyer,[§] Jan Balzarini,[∥] and Luigi A. Agrofoglio*[,‡]

[†]*Groupe d'Enzymologie Moléculaire et Fonctionnelle, UR4-UPMC, Université Pierre et Marie Curie, Sorbonne Universités, case courrier 256, 7, quai St Bernard, 75252 Paris Cedex 05, France,* [‡]*Institut de Chimie Organique et Analytique, Centre National de Recherche Scientifique Unité Mixte de Recherche 6005, Université d'Orléans, 45067 Orléans, France,* [§]*Laboratoire d'Enzymologie et Biochimie Structurales, Centre National de la Recherche Scientifique UPR 3082, 91198 Gif-sur-Yvette Cedex, France,* [∥]*REGA Institute for Medical Research, Katholieke Universiteit Leuven, Leuven, Belgium, and* [⊥]*Department of Veterinary Medical Chemistry, Swedish University of Agricultural Sciences, Box 575, Biomedical Center, S-751 24 Uppsala, Sweden.* [∞]*Both authors made equal contributions to this work.*

Received September 4, 2010

Acyclic nucleoside phosphonates (ANPs) are at the cornerstone of DNA virus and retrovirus therapies. They reach their target, the viral DNA polymerase, after two phosphorylation steps catalyzed by cellular kinases. New pyrimidine ANPs have been synthesized with unsaturated acyclic side chains (prop-2-enyl-, but-2-enyl-, pent-2-enyl-) and different substituents at the C5 position of the uracil nucleobase. Several derivatives in the but-2-enyl- series **9d** and **9e**, with (*E*) but not with (*Z*) configuration, were efficient substrates for human thymidine monophosphate (TMP) kinase, but not for uridine monophosphate−cytosine monophosphate (UMP-CMP) kinase, which is in contrast to cidofovir. Human TMP kinase was successfully crystallized in a complex with phosphorylated (*E*)-thymidine-but-2-enyl phosphonate **9e** and ADP. The bis-pivaloyloxymethyl (POM) esters of (*E*)-**9d** and (*E*)-**9e** were synthesized and shown to exert activity against herpes virus in vitro (IC_{50} = 3 μM) and against varicella zoster virus in vitro (IC_{50} = 0.19 μM), in contrast to the corresponding inactive (*Z*) derivatives. Thus, their antiviral activity correlates with their ability to act as thymidylate kinase substrates.

Introduction

In the past ten years, acyclic nucleoside phosphonates (ANPs), nucleotide analogues with a stable P−C bond, have become major antiviral nucleotide derivatives; three ANPs (adefovir [PMEA], tenofovir [(*R*)-PMPA], and cidofovir [(*S*)-CDV]) are approved for the treatment of severe viral infections (Figure 1).[1] The only acyclic pyrimidine nucleoside phosphonate analogue found to be effective to date is cidofovir (CDV) and the acyclic 2,4-diaminopyrimidine nucleoside phosphonates (i.e., PMEO-DAPym).[2] Their activities are based on the intracellular phosphorylation to their diphosphates (ANP-PPs), which act as a triphosphate, by two salvage pathway kinases (nucleoside monophosphate [NMP] and nucleoside diphosphate [NDP] kinases). The diphosphorylated ANPs act as chain terminators of virus DNA polymerase[3−6] inhibiting the viral (i.e., in HIV[7] or vaccinia) replication.[8,9] All studied ANPs are slowly phosphorylated by human NMP kinases: AMP kinases 1 and 2 for PMEA and (*R*)-PMPA,[3,10] and human UMP-CMP kinase (hUCK) for CDV.[4,11] The last phosphorylation step is performed by several enzymes, including NDP kinases and creatine kinases.[3,4] In order to improve the antiviral properties of ANPs, we have recently focused on the synthesis of new pyrimidine ANPs with the phosphorus atom attached to an unsaturated side chain and described a method of screening those ANPs for their affinity to act at the acceptor-binding site of hUCK.[11] (Note: PDB ID for the human TMP kinase complexed to (*E*)-TbutP and ADP: 2xx3.

Several novel (*E*)-3-(N^1-uracil)-prop-2-enyl phosphonic acid (U-proP, **6a**−**c**) derivatives were found to have similar affinities to the natural 2′-deoxyuridine monophosphate (dUMP) and 2′-deoxycytidine monophosphate (dCMP) substrates, and higher affinity than that of CDV; however, they were not substrates for hUCK.[11,12] Thus, we wanted to investigate the contribution, if any, of the length of the unsaturated chain of our derivatives (e.g., extending from a prop-2-enyl- to a but-2-enyl- or pent-2-enyl- side chain) to the efficiency of phosphorylation by human TMP kinase (hTMPK) and hUCK. Our rational design was based on the replacement of the O−C bond with a *trans*-alkene which would allow mimicry of the three-dimensional geometry provided by the backbone of PMEA, PMPA, and CDV while maintaining an electronic contribution similar to that brought by the oxygen atom.

From a chemical viewpoint, a general strategy for the convenient stereo-controlled synthesis of *trans*-alkene acyclic nucleoside phosphonates based on olefin cross metathesis seemed to be attractive, as the original approach tends to be tedious and low-yielding. Several new derivatives are efficiently activated by hTMPK, and the best substrates were converted to bis-(pivaloyloxymethyl)ester phosphonate prodrugs and found to be active against several herpes viruses in cell cultures.

*Corresponding authors. Luigi A. Agrofoglio, Phone +33 238-494-582, Fax + 33 238-471-281, E-mail: Luigi.Agrofoglio@univ-orleans.fr. Chahrazade El-Amri, Phone +33-144-276-952, Fax +331.44.27.51.40, E-mail: chahrazade.el_amri@upmc.fr.

 Published on Web 12/03/2010

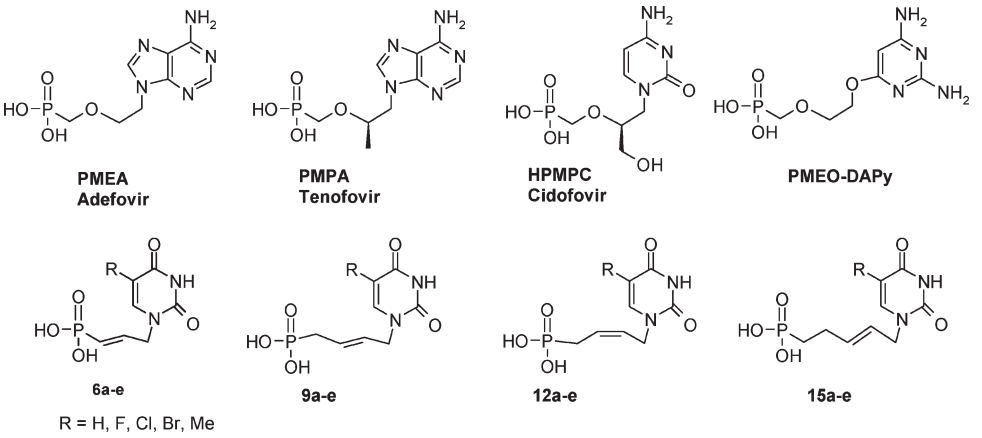

Figure 1. Structure of bioactive ANP and derivatives studied.

Scheme 1. Synthesis of Prop-2-enyl-, But-2-enyl-, and Pent-2-enyl- Acyclonucleoside Phosphonates[a]

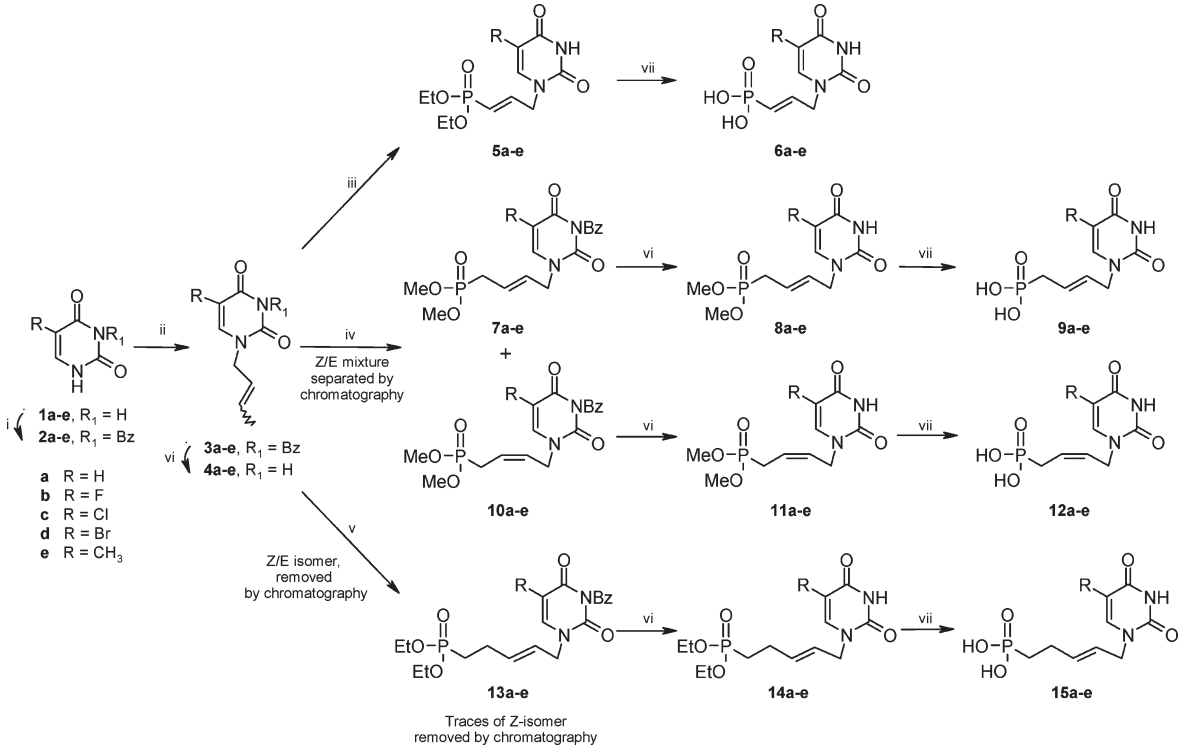

[a] Reagents and conditions: (i) BzCl, pyridine/CH_3CN; (ii) crotyl bromide, K_2CO_3, DMF; (iii) diethyl vinylphosphonate, [Ru] = cat., CH_2Cl_2, 40 °C; (iv) dimethyl allylphosphonate, [Ru] = cat., CH_2Cl_2, 40 °C; (v) diethyl but-3-enylphosphonate, [Ru] = cat., CH_2Cl_2, 40 °C; (vi) NH_3/MeOH; (vii) TMSBr, CH_2Cl_2.

Results and Discussion

Chemistry. The key step of olefin cross metathesis was realized between commercial alkenyl phosphonates and various C5-substituted-N^3-benzoylated crotylated uracils **3a**−**e** or unprotected analogues **4a**−**e** to prepare phosphonate derivatives **6a**−**e**, **9a**−**e**, **12a**−**e**, and **15a**−**e**, according to procedures previously described by our group (Scheme 1).[13] In agreement with the general model reported by Grubbs[14] for olefin cross metathesis, the use of crotylated building blocks promoted heterodimer formation while reducing the formation of homodimers, contrary to allylated derivatives.

Thus, starting from the appropriate C5-substituted uracil **1a**−**d** and thymine **1e**, a regioselective N^3-benzoylation[15] led to compounds **2a**−**e** and a subsequent alkylation with crotyl bromide afforded **3a**−**e**, respectively. A cross metathesis reaction between **3a**−**e** and dimethyl allylphosphonate catalyzed by the [Ru] = Grubbs II catalyst afforded a chromatographically separable mixture of (*E*)-but-2-enyl **7a**−**e** and the *Z* isomers **10a**−**e** (*E*/*Z*, 4:1). Removal of the benzoyl protecting group by 7 N NH_3/MeOH of compounds **7a**−**e** and **10a**−**e** afforded, respectively, derivatives (*E*)-**8a**−**e** and (*Z*)-**11a**−**e**. Subsequent cleavage of the phosphonic ester by TMSBr led to the free but-2-enyl-phosphonic acids (*E*)-**9a**−**e** and (*Z*)-**12a**−**e**, respectively. Under the same conditions of CM, **3a**−**e** was treated with diethyl but-3-enylphosphonate to afford the desired cross-coupling heterodimers (*E*)-**13a**−**e**, with only traces of (*Z*)-isomers. Subsequent deprotections afforded the free pent-2-enyl- phosphonic acid (*E*)-**15a**−**e**. From NH_3/MeOH deprotection **3a**−**e**, the cross-metathesis reaction between **4a**−**e** and an excess of vinyl diethylphosphonate was

Scheme 2. Synthesis of Bis(POM) Prodrugs of (*E*) and (*Z*) TbutP and 5Br-UbutP[a]

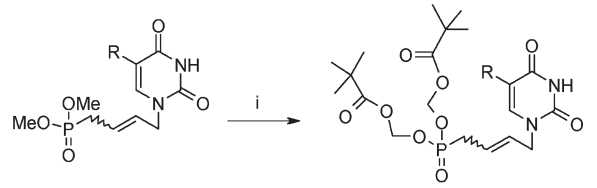

[a] Reagents and conditions: (i) chloromethyl pivalate, NaI, CH_3CN, reflux.

performed with Grubbs II catalyst. The desired cross-coupling heterodimers **5a**−**e** were obtained in moderate to good yields exclusively as the (*E*)-isomers. The stereochemistry of the olefin was confirmed by ^{1}H NMR, with a ^3J coupling constant (~17.0 Hz) of the olefinic protons. Upon treatment with TMSBr in CH_2Cl_2, the free prop-2-enyl- phosphonic acids **6a**−**e** were isolated in good yields. Finally, for cellular evaluation of the antiviral activity, the two best acid phosphonate substrates of hTMPK **9d**,**e** and **12d**,**e** were converted to their bis(POM) prodrugs by reaction of dimethyl phosphonate derivatives **8d**,**e** and **11d**,**e** with chloromethyl pivalate and sodium iodide (Scheme 2).[16] The following bis(POM)-ester prodrugs (*E*)-bis(POM)TbutP **16**, (*Z*)-bis(POM)TbutP **17**, (*E*)-bis(POM)-5Br-UbutP **18**, and (*Z*)-bis(POM)-5Br-UbutP **19** were obtained in moderate (for (*Z*)-isomers) to good yields (for (*E*)-isomers) (Scheme 2).

Reaction of C5-Substituted-Uracil ANP with Human hTMPK. The ability of new unsaturated ANPs (bearing a uracil, thymine, cytosine, or C5-halogeno-uracil moiety) to be phosphorylated by kinases present in human cells was measured first using an enzymatic in vitro assay with recombinant hTMPK.[17] TMPK was found associated with cell proliferation resulting in an expression peak in the S-phase of the cell cycle.[18] The recombinant forms of this "housekeeping" enzyme was already described and its substrate specificity and catalytic potency determined toward a large panel of substrates including antiviral compounds has been described.[17,19−21] Recently, a putative mitochondrial hTMPK has been reported.[22] However, it was not considered here, since it may be only a minor contributor to nucleoside analogue activation in cells.

Figure 2 represents the saturation curves for (*Z*)- and (*E*)-5-halouracil-but-2-enyl phosphonates as substrates with hTMPK in the presence of saturating ATP. All substrates show a hyperbolic saturation curve, indicating that they are all true Michaelis−Menten substrates. The rate constants of the (*E*)-isomers were better than those for the (*Z*)-derivatives, indicating that hTMPK worked better on butenyl-substrates with a *trans* configuration, as shown for UbutP **9a** and **12a**, 5F-UbutP **9b** and **12b**, 5Cl-UbutP **9c** and **12c**, and 5Br-UbutP **9d** and **12d** (Figure 2). This confirmed our hypothesis that replacement of O−C bond with *trans*-alkene would allow us to mimic the three-dimensional geometry provided by the backbone of ANP.

Thus, on the basis of saturation curves which indicate that only the (*E*)-isomers of the butenyl series are substrates for hTMPK, only the (*E*)-isomers of the newly obtained ANP were compared to natural 2′-deoxyribonucleotides monophosphate for their enzymatic properties (k_{cat}, K_M, and catalytic efficiency k_{cat}/K_M) toward human TMP kinase (Table 1).

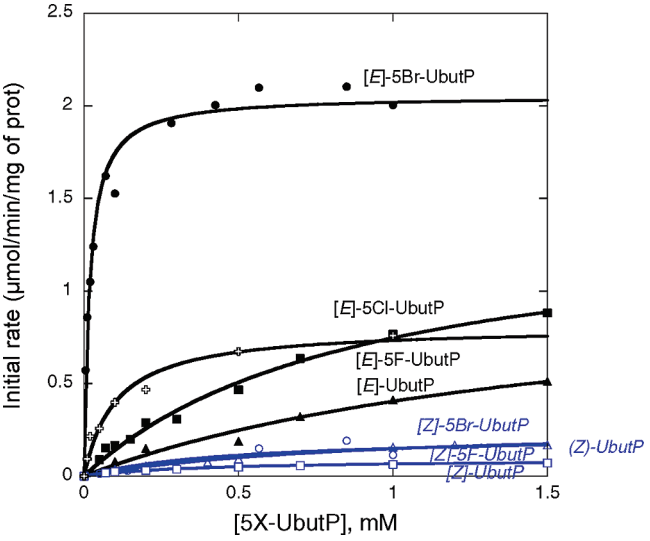

Figure 2. Treatment of human TMP kinase with (Z)- and (E)-5-halouracil-but-2-enyl-phosphonates. hTMPK saturation curves were plotted as a function of UbutP derivatives as substrates: (E)-UbutP **9a** (▲), (Z)-UbutP **12a** (△), (E)-5F-UbutP **9b** (■), (Z)-5F-UbutP **12b** (□), (E)-5Br-UbutP **9d** (●), (Z)-5Br-UbutP **12d** (○), and (E)-5Cl-UbutP **9c** (+). The initial rate of each acceptor phosphorylation was measured in the presence of 1 mM ATP and 5 mM Mg^{2+} using the standard coupled assay. The quantity of enzyme used in each experiment was 0.56 μM for (E)-5Br-UbutP (**9d**); 1.4 μM for (E)-5F-UbutP (**9b**), (E)-5Cl-UbutP (**9c**), and (E)-UbutP (**9a**); 2.8 μM for (Z)-UbutP (**12a**) and (Z)-5Br-UbutP (**12d**), 8.4 μM for (Z)-5F-UbutP (**12b**). K_M and k_{cat} values were obtained by fitting to a hyperbole (results shown in Table 1 for (*E*) stereoisomers). K_M and k_{cat} values were 0.55 mM and 0.12 s^{-1} for (Z)-UbutP **12a**; 0.3 mM and 0.037 s^{-1} for (Z)-5F-UbutP **12b**; 0.4 mM and 0.2 s^{-1} for (Z)-5Br-UbutP **12d**.

Michaelis constants K_M are rather similar to K_M^{TMP} within one order of magnitude. The presence of a halogen at the C5 position enhanced both the affinity and the turnover number. The best substrates for hTMPK in the (*E*)-butenyl series were the 5Br-UbutP **9d** and 5Me-UbutP (TbutP) **9e**, as their catalytic efficiencies (k_{cat}/K_M) were only found to be 3−4 times lower than the natural substrate TMP. Both (*E*)-prop-2-enyl- and (*E*)-pent-2-enyl analogues were less efficient substrates than their butenyl counterparts. The (*E*)-5Cl-UproP **6c** was slowly phosphorylated by hTMPK at low concentrations[11] and (*E*)-TproP ((*E*)-5Me-UproP, **6e**) was slightly better. The (*E*)-pentenyl- series was found to be more efficient with the best substrate being (*E*)-TpenP **15e** (Table 1, Figure 3). The histogram provided in Figure 3 clearly shows that (*E*)-5Br-UbutP **9d** and (*E*)-TbutP **9e** are phosphorylated by hTMPK at efficiencies similar to natural substrates, dUMP and TMP.

Crystal Structure of (*E*)-TbutP (9e) in hTMPK Active Site. The hTMPK fold was found to be highly similar to the adenylate kinase fold, with a CORE domain containing the ATP binding site, and two mobile domains, the NMP and LID domains, closing up upon substrate binding.[21] To establish and understand the structural basis for (*E*)-TbutP **9e** recognition and phosphorylation by the hTMPK, the structure of the hTMPK/(*E*)-TbutP **9e** co-crystal was solved, and details of the crystallographic data analysis are available (Supporting Information Table 1). The structure showed a phosphorylated TbutP molecule **9e** (TbutP-P) at the acceptor site of the enzyme and an ADP molecule at the donor site (Figure 4A). Since the crystals grew in the presence of TbutP

Table 1. Enzymatic Parameters for [*E*]-C5-Substituted Uracil Acyclic Phosphonates with Human TMP Kinase

	R	acronym	K_M (mM)	k_{cat} (s^{-1})	k_{cat}/K_M (M^{-1} s^{-1})
A- Propenyl	H-	**6a** (*E*)-UproP[a]	nd	nd	nd[a]
	F-	**6b** (*E*)-5F-UproP	nd	nd	nd
	Cl-	**6c** (*E*)-5Cl-UproP	nd	nd	80[a]
	Br-	**6d** (*E*)-5Br-UproP	nd	nd	nd[a]
	CH_3-	**6f** (*E*)-TproP	1	0.6	600
B- Butenyl	H-	**9a** (*E*)-UbutP	1.7	0.48	280
	F-	**9b** (*E*)-5F-UbutP	1	0.73	730
	Cl-	**9c** (*E*)-5Cl-UbutP	0.13	0.50	4100
	Br-	**9d** (*E*)-5Br-UbutP	0.02	0.90	45 000
	CH_3-	**9e** (*E*)-TbutP	0.024	0.84	35 000
C-Pentenyl	H-	**15a** (*E*)-UpenP	2.5	0.074	30
	F-	**15b** (*E*)-5F-UpenP	1.9	0.09	47
	Cl-	**15c** (*E*)-5Cl-UpenP	0.15	0.1	660
	Br-	**15d** (*E*)-5Br-UpenP	0.16	0.058	360
	CH_3-	**15e** (*E*)-TpenP	0.10	0.32	3200
references		dUMP	0.17[b]	4.8[b]	28 000[b]
		dTMP	0.02[b]	3[b]	150 000[b]
		5Br-dUMP	0.01	1.2	120 000
		AZTMP			1000[c]
		cidofovir	nd	nd	nd

[a] Ref 11. [b] Ref 17. [c] Ref 21. nd: not detectable, standard error 15%.

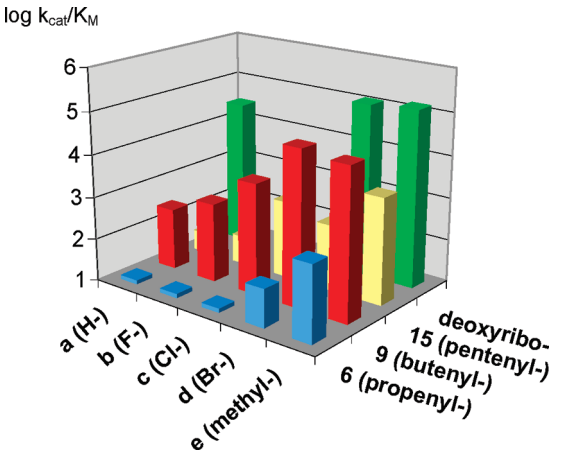

Figure 3. Histogram of human TMP kinase phosphotransfer efficiency with synthesized (*E*)-unsaturated ANP. The kinetic parameters of pure recombinant hTMPK were measured at the steady state. Catalytic efficiencies were calculated from the ratio k_{cat}/K_M and expressed as M^{-1} s^{-1}. O*y* axis: blue, propenyl series; red, butenyl series; yellow, pentenyl series; and green, 2′-deoxyriboses (standard). O*x* axis: substitutions at C5 position: H, F, Cl, Br, and CH_3.

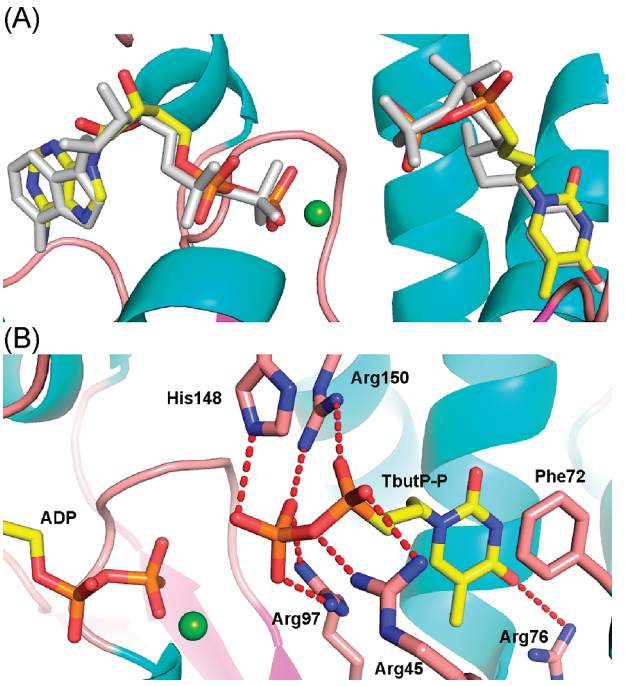

Figure 4. Crystal structure of human TMP kinase complexed to (E)-TbutP **9e** and ADP. (A) X-ray crystal structure of the (E)-TbutP (**9e**) molecule bound to the human TMP kinase enzyme (cartoon with cyan helices and pink loops). (E)-TbutP is phosphorylated and the phosphate donor site is occupied by ADP (atom type color) and Mg^{2+} (green). The structure of the natural substrates dTDP and ADP (gray) bound to the enzyme are superimposed (PDB ID 1e2g). (B) Key active site residues involved in TButP-P recognition are labeled, and the polar interactions made with the nucleotide analog are shown by red dashes.

and ATP, the phosphoryl transfer must have taken place during crystallization.

We compared TbutP-P with the natural substrate TDP from the hTMPK/TDP/ADP structure.[21] The (E)-but-2-enyl side chain moiety mimics the conformation of the C1′-O4′-C4′-C5′ atoms from the 2′-deoxyribose in TDP, confirming our hypothesis. The phosphorylated TbutP-P derivative was slightly shifted toward the phosphate site so that its phosphonate and phosphate are almost superimposed with the α and *β*-phosphate of TDP. As a consequence of the lack of a 3′-hydroxyl, the interaction with Asp15 is lost, and the enzyme LID conformation is rearranged in such a manner that Arg150 is reoriented and occupies this leaving space. Consequently, Arg150 together with His148 strongly interacts with the TbutP-P phosphonate and phosphate (Figure 4B), allowing a productive binding of TbutP-P and ADP in hTMPK active site.

C5-Substituted-Uracil ANP as Potential Ligands of hUCK, hTK1, and hTK2. As mentioned above, the synthesized C5-substituted-uracil unsaturated ANPs were assayed with different human kinases compatible with their structures (hUCK, thymidine kinases 1 and 2) allowing their recognition by the enzymes. All uracil unsaturated ANPs were not substrates of hUCK, regardless of the unsaturated acyclic

Table 2. Antiviral Activities and Cytotoxicities in HEL Cell Cultures of Bis(POM) Prodrugs of (*E*) and (*Z*) TbutP **16** and **17** and 5Br-UbutP **18** and **19**

			EC_{50}[a] (μM)						
			HSV-1	HSV-2	HSV-1 TK^-	Vaccinia virus	HCMV	VZV	
compound	CC_{50}[b]	MCC[c]	(KOS)	(G)	(KOS ACV^r)		(AD-169 and Davis)	TK^+ (OKA)	TK^- (07/1)
[*E*]-bis(POM)-TbutP (**16**)	35	≥200	3.1	6.1	9.2	30	>40	0.41	0.19
[*Z*]-bis(POM)-TbutP (**17**)	35	≥200	>40	>40	>40	>40	>200	>40	>40
[*E*]-bis(POM)-5Br-UbutP (**18**)	34	200	20	16	19	33	>40	20	15
[*Z*]-bis(POM)-5Br-UbutP (**19**)	70	>200	>200	45	>200	90	>200	97	110
Brivudin	>250	>250	0.04	30	250	1.5	>250	0.012	>100
Cidofovir	280	>250	3.5	2.0	2.5	6.0	1.2	0.044	0.070
Ganciclovir	164	>100	0.08	0.05	3.0	>100	5.2	3.3[d]	62[d]

[a] Effective concentration (μM), required to reduce virus-induced cytopathogenicity by 50%. [b] Cytostatic concentration (μM), required to inhibit HEL cell proliferation by 50%. [c] Minimum cytotoxic concentration (μM), required to cause a microscopically detectable alteration of normal cell morphology. [d] Data for acyclovir (μM).

chain, but inhibitors for some of them (e.g., **9c**), (Supporting Information Figure 1). This is in contrast to CDV, which is slowly processed to CDV-phosphate by hUCK.[4,11] Spectroscopic experiments using circular dichroism also indicate that the new phosphonates described here do not induce the conformation change induced by dCMP and cidofovir (Supporting Information Table 2).

The ability of the most promising hTMPK substrates to inhibit hUCK activity was investigated. (*E*)-TbutP **9e** and (*E*)-5Cl-UbutP **9c** were both found to be poor inhibitors (K_I = 1.2 mM and 0.25 mM, respectively). Surprisingly, **9c** was found to bind to both sites (dCMP and ATP sites) of hUCK, thus preventing any substrate activity (Supporting Information Figure 1A,B). The binding to the ATP site was confirmed by fluorescence competition assay with *N*-methyl anthraniloyl ATP (Mant-ATP) as probe.[11,23] Compound **9c** readily displaced Mant-ATP ($^{app}K_D$ = 0.17 mM). CDP-β-(*N*′-methylanthraniloylaminobutyl)-phosphoramidate (MABA-CDP) was also displaced by **9c**, indicating that it also binds to the acceptor site (dCMP site) with an apparent equilibrium dissociation constant K_D = 0.16 mM.[11] The affinity constants measured by fluorophore displacement were in the same range as the K_I obtained from kinetic inhibition data, any differences being presumably due to the bulky Mant-moiety. It is important to note that CDV, PMEA, and PMPA did not displace Mant-ATP from hUCK, showing that they do not bind to the ATP site. Similarly, the new acyclic compounds also did not displace Mant-ATP from the ATP site of hTMPK.

Several acyclic nucleoside analogues have been previously shown to inhibit mitochondrial thymidine kinase (TK).[24] So, the possible inhibition of human recombinant TK1 (cytosolic) and TK2 (mitochondrial) by (*E*)-5Cl-UbutP **9c** has been investigated. At the concentration of 0.3 mM, **9c** proved to inhibit thymidine phosphorylation (1 μM) catalyzed by TK1 and TK2 (ATP 1 mM and thymidine 0.3 mM) by less than 15% activity. Altogether, these data rule out a strong interaction of the C5-substituted-uracil-unsaturated ANP with TK1 and TK2, as well as with hUCK. They most likely will not be recognized by these enzymes in the cell context, as the cellular concentration of ANP rarely reaches a concentration such as 0.3 mM.

Antiviral Activities of Selected Novel Pyrimidine Unsaturated ANP in HEL Cell Cultures. The newly synthesized compounds were evaluated against a variety of DNA viruses including herpes simplex virus type 1 (HSV-1, strain KOS), HSV-2 (strain G), thymidine kinase (TK)-deficient HSV-1 TK^-, varicella zoster virus (VZV, strain OKA), TK-deficient VZV TK^- (07/1), human cytomegalovirus (HCMV), and vaccinia virus (VV) in HEL cell cultures. All derivatives were devoid of antiviral activity except when the phosphonate group was protected by POM groups (Table 2). This lack of activity confirms the low biodisponibility of acid phosphonates and the need of a biolabile protecting group to reveal antiviral activities.

The bis(POM) derivative of (*E*)-TbutP **16** showed pronounced inhibitory activity against HSV-1, HSV-2, and VZV (EC_{50} = 2.5−6.1 μM). Interestingly, the compound showed comparable antiviral activity against TK^- deficient virus strains with a decreased inhibitory effect (EC_{50} = 9.2 μM) against the TK^- deficient HSV-1 strain, but an excellent increase in activity against the VZV TK^- strain with EC_{50} = 0.19 μM. There was moderate antiviral activity against VV replication, but no activity against HCMV. Also, (*E*)-bis(POM)-5Br-UbutP **18** proved to be inhibitory against HSV-1, HSV-2, VZV, and VV, but not HCMV (EC_{50} = 16−33 μM) and fully kept activity against HSV-1 TK^- and VZV TK^-. The compounds were not significantly cytotoxic at 200 μM, but slightly cytostatic at 34−70 μM against HEL cell proliferation. In contrast with the (*E*) isomer of bis(POM)-TbutP **16** and bis(POM)-UbutP **18**, the corresponding (*Z*) isomers **17** and **19** exhibited little or no antiviral activity.

The (*E*)-bis(POM)-TbutP derivative **16** proved most inhibitory against HSV-1, HSV-2, and VZV. Presumably, in analogy to bis(POM)-PMEA, the compound was rapidly taken up by the virus-infected cells and intracellularly converted to the free phosphonate derivative after hydrolysis of the POM prodrug moieties by cellular esterases. In this way, it circumvented the HSV-1 TK dependency of pyrimidine nucleoside analogues such as brivudin (BVDU) for further conversion to its active metabolite. The independence of cellular TK activity was testified by the pronounced antiviral activity of the compound against mutant TK-deficient HSV-1 TK^- and VZV TK^-. As is also the case for other phosphonates such as PMPA and CDV, the nature of the isomers [(*R*) or (*S*) for PMPA/CDV or (*E*) or (*Z*) for bis(POM)-TbutP] is important for its eventual antiviral activity. The higher antiviral activity of the (*E*) enantiomers **16** and **18** compared to the corresponding (*Z*) isomers **17** and **19** clearly correlated with their ability to be phosphorylated by hTMPK. This is an argument in favor of a mode of action involving phosphorylation of the compounds in the host cells in order to target virus DNA polymerase. It is remarkable that Hostetler's group recently reported the antiviral activity of similar pentenyl derivatives of uracil and thymine against several DNA viruses and hepatitis B virus, but in (*Z*) configuration, when assayed as hexadecyloxy-propyl esters to increase their penetration into cells.[25] Indeed, (*E*)-TbutP

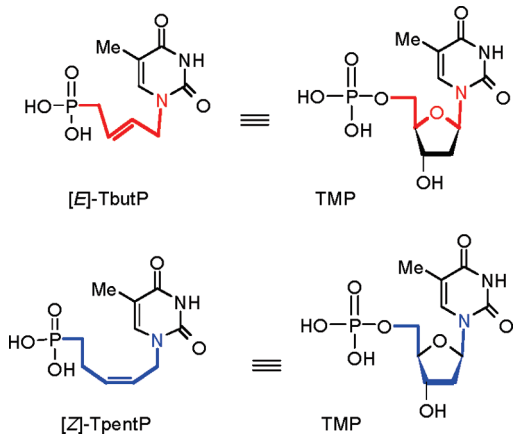

Figure 5. Structural comparison of (*E*)-TbutP and (*Z*)-TpentP as nonclassical bioisosters of TMP.

with a 4-carbon acyclic moiety (butenyl series) in trans configuration and (*Z*)-TpentP in cis configuration both mimic TMP and can be considered as nonclassical bioisosters for hTMPK. They both adopt a similar conformation to the natural substrate TMP (Figure 5): the side chain of (*E*)-TbutP mimic atoms C1′-O4′-C4′-C5′ of TMP (skeleton in red), as shown from the crystal structure, whereas the side chain of (*Z*)-TpentP mimic atoms C1′-C2′-C3′-C4′-C5′ of TMP (skeleton in blue). (*Z*)-TpenP and (*Z*)-UpenP are then likely efficient substrates for hTMPK.

Conclusion

In the present study, from several new compound acyclonucleoside phosphonates, the (*E*)-thymidine-but-2-enyl phosphonate **9e** was markedly phosphorylated by recombinant hTMPK with efficiency reaching more than twenty times that of AZT-monophosphate. We have demonstrated by X-ray analysis of (*E*)-TbutP **9e** in hTMPK that the (*E*)-unsaturated chain moiety mimics the conformation of the C1′-04′-C4′-C5′ atoms from the 2′-deoxyribose in TDP The bis(POM) prodrug of (*E*)-TbutP **16** presented a potent antiviral activity in vitro against several herpes viruses, namely, herpes simplex viruses 1 and 2 and varicella zoster virus. Its C5-substituted analogues were also substrates for hTMPK with efficiencies strongly dependent on the nature of the C5-substituent but with weaker antiviral activities. The (*E*)-bis(POM)-TbutP **16** derivative should be considered a novel antiviral lead compound for further optimization of both activation by cellular and viral kinases and antiviral potencies. Particularly, interactions of the ANPs with the ATP site of human UMP-CMP kinase have to be considered and avoided in the design of future effective compounds.

Experimental Section

Chemistry. Natural nucleotides were purchased from Sigma Chemicals (St. Louis, MO, USA) and Mant-ATP from Jena Biosciences (Jena, Germany). MABA-TDP and MABA-CDP were kindly synthesized by Dr. S. Pochet (Institut Pasteur, Paris) as described.[11,26] Commercially available chemicals were used as received. CH_2Cl_2 was distilled from CaH_2 prior to use. Reactions were monitored by thin-layer chromatography (TLC) analysis using silica gel plates (Kieselgel 60 F_{254}). Compounds were visualized by UV irradiation and/or spraying with water solution of potassium permanganate $KMnO_4$, followed by charring at 150 °C. Column chromatography was performed on silica gel 60 M (0.040−0.063 mm). ^{1}H NMR spectra were recorded on 250 or 400 MHz spectrometers, ^{13}C NMR on 62.9 or 100 MHz spectrometers, and ^{31}P on 162 MHz spectrometer at room temperature, using deuterated solvents as internal standard. Chemical shifts are given in ppm and multiplicities are reported as s (singlet), d (doublet), t (triplet), q (quartet), q_i (quintuplet), or m (multiplet). Assignments of NMR spectra follow standard nucleosides nomenclature: nucleoside bases are numbered from *N*-1 to *C*-6 and acyclic chains are numbered from *C*-1′ to *C*-5′. Similar conventions apply for the corresponding hydrogen atoms. High-resolution mass spectrometry was performed by the Mass Spectrometry Center of Blaise Pascal University (Aubière, France). The purity was determined by semipreparative HPLC (Hypersil 100; C-18; 5 μm); with an appropriate gradient of acetonitrile/H_2O; purity of key target compounds was >95%.

The following products are known products or previously reported by our group:[14] N^3-Benzoyluracil (**2a**), CAS registration 2775−87−3; N^3-Benzoyl-5-fluorouracil (**2b**), CAS registration 61251−77−2; N^3-Benzoyl-5-chlorouracil (**2c**), CAS registration 214687−03−3; N^3-Benzoyl-5-bromouracil (**2d**), CAS registration 206762−91−6; N^3-Benzoylthymine (**2e**), CAS registration 4330−20−5; N^3-Benzoyl-N^1-crotyluracil (**3a**), CAS registration 1067228−36−7; N^3-Benzoyl-N^1-crotyl-5-chlorouracil (**3c**), CAS registration 1023339−53−8; N^3-Benzoyl-N^1-crotyl-5-bromouracil (**3d**), CAS registration 1023339−58−3; N^3-Benzoyl-N^1-crotylthymine (**3e**), CAS registration 882659−57−6; N^1-Crotyluracil (**4a**), CAS registration 852998−43−7; N^1-[(*E*)-3-Diethoxyphosphonyl-prop-2-enyl]-uracil (**5a**), CAS registration 1023339−16−3; N^1-[(*E*)-3-Diethoxyphosphonyl-prop-2-enyl]-5-chlorouracil (**5c**), CAS registration 1023339−72−1; N^1-[(*E*)-3-Diethoxyphosphonyl-prop-2-enyl]-5-bromouracil (**5d**), CAS registration 1023339−74−3; N^1-[(*E*)-3-Dihydroxyphosphonyl-prop-2-enyl]-uracil (**6a**), CAS registration 1023339−19−6; N^1-[(*E*)-3-Dihydroxyphosphonyl-prop-2-enyl]-5-chlorouracil (**6c**), CAS registration 1023339−96−9; N^1-[(*E*)-3-Dihydroxyphosphonyl-prop-2-enyl]-5-bromouracil (**6d**), CAS registration 1023339−98−1; N^3-Benzoyl-N^1-[(*E*)-4-dimethoxyphosphonylbut-2-enyl]-uracil (**7a**), CAS registration 1023339−30−1; N^3-Benzoyl-N^1-[(*E*)-4-dimethoxyphosphonylbut-2-enyl]-5-chlorouracil (**7c**), CAS registration 1023339−83−4; N^3-Benzoyl-N^1-[(*E*)-4-dimethoxyphosphonylbut-2-enyl]-5-bromouracil (**7d**), CAS registration 1023339−86−7; N^1-[(*E*)-4-Dihydroxyphosphonyl-but-2-enyl]-uracil (**9a**), CAS registration 1023339−32−3; N^1-[(*E*)-4-Dihydroxyphosphonyl-but-2-enyl]-5-chlorouracil (**9c**), CAS registration 1023340−06−8; N^1-[(*E*)-4-Dihydroxyphosphonyl-but-2-enyl]-5-bromouracil (**9d**), CAS registration 1023340−07−9; N^3-Benzoyl-N^1-[(*Z*)-4-dimethoxyphosphonylbut-2-enyl]-uracil (**10a**), CAS registration 1023339−30−1; N^3-Benzoyl-N^1-[(*Z*)-4-dimethoxyphosphonyl-but-2-enyl]-5-chlorouracil (**10c**), CAS registration 1023340−16−0; N^3-Benzoyl-N^1-[(*Z*)-4-dimethoxyphosphonyl-but-2-enyl]-5-bromouracil (**10d**), CAS registration 1023340−17−1; N^1-[(*Z*)-4-Dihydroxyphosphonyl-but-2-enyl]-uracil (**12a**), CAS registration 1023339−34−5; N^1-[(*Z*)-4-Dihydroxyphosphonyl-but-2-enyl]-5-chlorouracil (**12c**), CAS registration 1173147−85−7.

N^3-Benzoyl-5-fluoro-N^1-crotyluracil (3b). To a DMF (12 mL) solution of N^3-benzoyl 5-fluoro-uracil (1.0 g) were added K_2CO_3 (1.05 equiv) and crotyl bromide (1.05 equiv) under argon atmosphere. After 1 h stirring at room temperature, the reaction mixture was diluted with EtOAc and then washed with an aqueous saturated NH_4Cl solution. The aqueous phases were extracted with EtOAc, and the combined organic layers were dried over $MgSO_4$, filtered, and concentrated under reduced pressure. The residue was purified by silica gel column chromatography (petroleum ether/EtOAc 5:5). HRMS (ESI): *m*/*z* calcd for $C_{15}H_{13}FN_2O_3Na$ ($M^+ + Na$) 311.0796, found 311.0792. ^{1}H NMR (400 MHz, $CDCl_3$): δ 7.92 (d, J = 8.0 Hz, 2H), 7.64 (t, J = 8.0 Hz, 1H), 7.51 (t, J = 8.0 Hz, 2H), 7.35 (d, 1H), 5.96−5.74 (m, 1H), 5.59−5.42 (m, 1H), 4.40 (d, J = 6.5 Hz, 0.4H), 4.29 (d, J = 6.5 Hz, 1.6H), 1.78 (d, J = 6.5 Hz, 3H).

General Procedure for Deprotection of N^3-Benzoylated-N^1-crotyluracil Analogues. The debenzoylation of N^3-benzoyl-N^1-crotyl-C5-substituted uracil (100 mg) was carried out at 4 °C overnight in a methanol solution 7 N of ammonia (5 mL). After evaporation of all the volatiles, the residue was purified by chromatography on silica gel (petroleum ether/EtOAc 50:50) to yield the desired compound, as a white solid. Following this general procedure, analogues **4a**−**e** were prepared and characterized as follows.

N^1-Crotyl-5-fluorouracil (4b). Yield: 89% (major/minor ratio = 70:30). Mp = 90 °C. ^{1}H NMR (400 MHz, $CDCl_3$): δ 10.96 (s, 1H), 7.35 (d, J = 5.7 Hz, 1H major), 7.27 (d, J = 5.7 Hz, 1H minor), 5.89−5.77 (m, 1H), 5.54−5.45 (m, 1H), 4.40 (d, J = 7.2 Hz, 2H minor), 4.30 (d, J = 6.6 Hz, 2H major), 1.77−1.73 (m, 3H).

N^1-Crotyl-5-chlorouracil (4c). Yield: 99% (major/minor ratio = 70:30). Mp = 142 °C. ^{1}H NMR (250 MHz, $CDCl_3$): δ 11.43 (s, 1H), 7.49 (s, 1H major), 7.39 (s, 1H minor), 5.93−5.73 (m, 1H), 5.56−5.28 (m, 1H), 4.40 (d, J = 7.5 Hz, 2H minor), 4.28 (d, J = 7.5 Hz, 2H major), 1.79−1.74 (m, 3H). HRMS (ESI): m/z calcd for $[M+H]^+$ $C_8H_9ClN_2O_2$ 200.6240, found 200.6242.

N^1-Crotyl-5-bromouracil (4d). Yield: 99% (major/minor ratio = 70:30). Mp = 144 °C. ^{1}H NMR (250 MHz, $CDCl_3$): δ 8.96 (s, 1H), 7.51 (s, 1H major), 7.48 (s, 1H minor), 5.90−5.75 (m, 1H), 5.56−5.43 (m, 1H), 4.42 (d, J = 7.2 Hz, 2H minor), 4.30 (d, J = 6.6 Hz, 2H major), 1.78−1.75 (m, 3H). MS (ESI): m/z calcd for $[M+H]^+$ $C_8H_9BrN_2O_2$ 245.0753, found 245.0757.

N^1-Crotylthymine (4e). Yield: 92% (major/minor ratio = 70:30). Mp = 110 °C. ^{1}H NMR (400 MHz, $CDCl_3$): δ 10.48 (s, 1H), 7.04 (dd, J = 5.6, 1.1 Hz, 1H), 5.78−5−69 (m, 1H major), 5.78−5−69 (m, 1H minor), 5.56−5.49 (m, 1H major), 5.45−5.39 (m, 1H minor), 4.57 (d, J = 6.7 Hz, 2H minor), 4.30 (d, J = 6.1 Hz, 2H major), 1.91 (s, 3H), 1.79 (d, J = 6.4 Hz, 3H major), 1.65 (d, J = 6.1 Hz, 3H minor).

General Procedure for Cross Coupling Metathesis.[14]. A mixture of N^3-benzoyl-N^1-crotyl-C5-substituted uracil, an appropriate alkenyl phosphonate [diethyl vinylphosphonate (4 equiv), dimethyl allylphosphonate (4 equiv), or diethyl but-2-enylphosphonate (2 equiv)] and [Ru] = Grubbs second generation catalyst (5% mol) was stirred in dry CH_2Cl_2 (5−10 mL) at 40 °C for 16 h under positive pressure of dry argon. After evaporation of all volatiles, the residue was purified by chromatography on silica gel with an elution gradient of EtOAc/MeOH to yield the desired compound as an oil. Following this general procedure, analogues **5a**−**e**, **7a**−**e**, **10a**−**e**, and **13a**−**e** were prepared and characterized as follows.

N^1-[(*E*)-3-Diethoxyphosphonyl-prop-2-enyl]-5-fluorouracil (5b). Yield: 47%. HRMS (ESI): m/z calcd for $C_{11}H_{17}N_2O_5FP$ $[M+H]^+$ 307.0859, found 307.0850. ^{1}H NMR (250 MHz, $CDCl_3$): δ 7.80 (d, 1H, J = 6.2 Hz, H^6), 6.73 (ddt, 1H, J = 4.8, 17.5, and 22.0 Hz, $H^{3\prime}$), 5.88 (tt, 1H, J = 1.8, 17.5 Hz, $H^{2\prime}$), 4.50 (m, 2H, $H^{1\prime}$), 4.04−4.11 (m, 4H, O-CH_2-CH_3), 1.31 (t, 6H J = 7.0 Hz, O-CH_2-CH_3). ^{31}P NMR (161.9 MHz, $CDCl_3$): δ 30.37.

N^1-[(*E*)-3-Diethoxyphosphonyl-prop-2-enyl]-thymine (5e). Yield: 54%. HRMS (ESI): m/z calcd for $C_{12}H_{20}N_2O_5P$ $[M+H]^+$ 303.1110, found 303.1109. ^{1}H NMR (400 MHz, $CDCl_3$): δ 9.31 (s, 1H), 6.89 (d, J = 1.2 Hz, 1H), 6.68 (ddt, J = 4.8, 17.2, and 21.6 Hz, 1H), 5.74 (tt, J = 1.8, 17.6 Hz, 1H), 4.44 (ddd, J = 1.8, 2.8, and 4.8 Hz, 2H), 4.02−4.10 (m, 4H), 1.86 (d, J = 1.2 Hz, 3H), 1.29 (t, J = 7.2 Hz, 6H). ^{31}P NMR (162 MHz, $CDCl_3$): δ 26.18.

N^3-Benzoyl-N^1-[(*E*)-4-dimethoxyphosphonylbut-2-enyl]-5-fluorouracil (7b). Yield: 72%. HRMS (ESI): m/z calcd for $C_{17}H_{18}N_2O_6FNaP$ $[M+H]^+$ 419.0784, found 419.0769. ^{1}H NMR (400 MHz, $CDCl_3$): δ 7.94−8.00 (m, 3H), 7.63 (t, J = 7.2 Hz, 1H), 7.51 (t, J = 8.0 Hz, 2H), 5.72−5.85 (m, 2H), 3.74 (m, 2H), 3.72 (d, J = 11.2 Hz, 6H), 2.74 (dd, J = 6.0, 22.0 Hz, 2H). ^{31}P NMR (162 MHz, $CDCl_3$): δ 34.25.

N^3-Benzoyl-N^1-[(*E*)-4-dimethoxyphosphonylbut-2-enyl]-thymine (7e). Yield: 60%. HRMS (ESI): m/z calcd for $C_{18}H_{22}N_2O_6P$ $[M+H]^+$ 393.1216, found 393.1232. ^{1}H NMR (400 MHz, $CDCl_3$): δ 7.87 (m, 2H), 7.61 (m, 1H), 7.46 (m, 2H), 7.09 (d, J = 1.2 Hz, 1H), 5.64−5.79 (m, 2H), 4.29 (m, 2H), 3.71 (d, J = 10.9 Hz, 6H), 2.61 (dd, J = 5.9, 21.4 Hz, 2H), 1.91 (d, J = 1.2 Hz, 3H). ^{31}P NMR (162 MHz, $CDCl_3$): δ 28.552.

N^3-Benzoyl-N^1-[(*Z*)-4-dimethoxyphosphonyl-but-2-enyl]-5-fluorouracil (10b). Yield: 17%. HRMS (ESI): m/z calcd for $C_{17}H_{18}N_2O_6FNaP$ $[M+H]^+$ 419.0784, found 419.0763. ^{1}H NMR (400 MHz, $CDCl_3$): δ 7.82−7.90 (m, 3H), 7.63 (tt, J = 2.0, 12.4 Hz, 1H), 7.51 (t, J = 12.4 Hz, 2H), 5.60−5.81 (m, 2H), 4.41 (dd, J = 6.0, 10.8 Hz, 2H), 3.72 (d, J = 17.6 Hz, 6H), 2.69 (dd, J = 11.2, 36.0 Hz, 2H). ^{31}P NMR (162 MHz, $CDCl_3$): δ 34.32.

N^3-Benzoyl-N^1-[(*Z*)-4-dimethoxyphosphonylbut-2-enyl]-thymine (10e). Yield: 13%. HRMS (ESI): m/z calcd for $C_{18}H_{21}N_2O_6NaP$ $[M+H]^+$ 415.1035, found 415.1040. ^{1}H NMR (250 MHz, $CDCl_3$): δ 7.90 (dd, J = 1.2, 8.2 Hz, 2H), 7.62 (m, 1H), 7.47 (t, J = 8.2 Hz, 2H), 7.34 (d, J = 0.8 Hz, 1H), 5.63−5.79 (m, 2H), 4.43 (m, 2H), 3.74 (d, J = 10.9 Hz, 6H), 2.74 (dd, J = 6.9, 22.3 Hz, 2H), 1.93 (s, 3H). ^{31}P NMR (162 MHz, $CDCl_3$): δ 28.557.

N^3-Benzoyl-N^1-[(*E*)-5-diethoxyphosphonyl-pent-2-enyl]-uracil (13a). Yield: 86%. HRMS (ESI): m/z calcd for $C_{20}H_{25}N_2O_6NaP$ $[M+H]^+$ 443.1348, found 443.1352. ^{1}H NMR (250 MHz, $CDCl_3$): δ 7.91 (d, J = 7.5 Hz, 2H), 7.64 (t, J = 7.5 Hz, 1H), 7.48 (t, J = 7.5 Hz, 2H), 7.30 (d, J = 8.0 Hz, 1H), 5.88−5.76 (m, 1H), 5.80 (d, J = 8.0 Hz, 1H), 5.57 (dt, J = 6.4, 15.2 Hz, 1H), 4.31 (d, J = 6.4 Hz, 2H), 4.15−4.02 (m, 4H), 2.44−2.35 (m, 2H), 1.86−1.77 (m, 2H), 1.31 (t, J = 6.8 Hz, 6H). ^{31}P NMR (162 MHz, $CDCl_3$): δ 30.57.

N^3-Benzoyl-N^1-[(*E*)-5-diethoxyphosphonyl-pent-2-enyl]-5-fluorouracil (13b). Yield: 78%. HRMS (ESI): m/z calcd for $C_{20}H_{24}FN_2O_6NaP$ $[M+H]^+$ 461.1254, found 461.1243. ^{1}H NMR (250 MHz, $CDCl_3$): δ 7.95 (d, J = 7.2 Hz, 2H), 7.70 (t, J = 7.6 Hz, 1H), 7.54 (t, J = 7.6 Hz, 2H), 7.48 (d, J = 5.6 Hz, 1H), 5.82 (dt, J = 6.4, 15.2 Hz, 1H), 5.52 (dt, J = 5.2, 16.8 Hz, 1H), 4.34 (d, J = 6.4 Hz, 2H), 4.08−4.20 (m, 4H), 2.38−2.55 (m, 2H), 182−1.92 (m, 2H), 1.27 (t, J = 7.2 Hz, 6H). ^{31}P NMR (162 MHz, $CDCl_3$): δ 30.43.

N^3-Benzoyl-N^1-[(*E*)-5-diethoxyphosphonyl-pent-2-enyl]-5-chlorouracil (13c). Yield: 69%. HRMS (ESI): m/z calcd for $C_{20}H_{24}ClN_2O_6NaP$ $[M+H]^+$ 477.0958, found 477.0937. ^{1}H NMR (250 MHz, $CDCl_3$): δ 7.89 (d, J = 7.5 Hz, 2H), 7.65 (t, J = 7.5 Hz, 1H), 7.57 (s, 1H), 7.53−7.45 (m, 2H), 5.86 (dt, J = 6.5, 15.0 Hz, 1H), 5.55 (dt, J = 6.5, 15.0 Hz, 1H), 4.31 (d, J = 6.5 Hz, 2H), 4.14−4.02 (m, 4H), 2.46−2.32 (m, 2H), 1.88−1.75 (m, 2H), 1.30 (t, J = 7.0 Hz, 6H). ^{31}P NMR (162 MHz, $CDCl_3$): δ 33.53.

N^3-Benzoyl-N^1-[(*E*)-5-diethoxyphosphonyl-pent-2-enyl]-5-bromouracil (13d). Yield: 80%. HRMS (ESI): m/z calcd for $C_{20}H_{24}BrN_2NaO_6P$ $[M+H]^+$ 521.0480, found 521.0483. ^{1}H NMR (400 MHz, $CDCl_3$): δ 7.87 (d, J = 7.2 Hz, 2H), 7.67 (s, 1H), 7.63 (t, J = 7.2 Hz, 1H), 7.46 (t, J = 7.5 Hz, 2H), 5.85 (dt, J = 6.4, 15.2 Hz, 1H), 5.53 (dt, J = 6.4, 15.2 Hz, 1H), 4.29 (d, J = 6.4 Hz, 2H), 4.13−4.00 (m, 4H), 2.41−2.32 (m, 2H), 1.84−1.76 (m, 2H), 1.29 (t, J = 7.0 Hz, 6H). ^{31}P NMR (162 MHz, $CDCl_3$): δ 30.49.

N^3-Benzoyl-N^1-[(*E*)-5-diethoxyphosphonyl-pent-2-enyl]-thymine (13e). Yield: 64%. HRMS (ESI): m/z calcd for $C_{21}H_{27}N_2NaO_6P$ $[M+H]^+$ 457.1504, found 457.1501. ^{1}H NMR (250 MHz, $CDCl_3$): δ 7.90 (d, J = 7.6 Hz, 2H), 7.63 (t, J = 7.6 Hz, 1H), 7.48 (t, J = 7.6 Hz, 2H), 7.12 (s, 1H), 5.73 (dt, J = 6.8, 15.2 Hz, 1H), 4.30 (d, J = 6.4 Hz, 2H), 5.52 (dt, J = 6.4, 15.2 Hz, 1H), 4.03−4.17 (m, 4H), 2.34−2.78 (m, 2H), 1.95 (s, 3H), 1.78−1.89 (m, 2H), 1.32 (t, J = 7.2 Hz, 6H). ^{31}P NMR (162 MHz, $CDCl_3$): δ 30.63.

General Procedure for the Deprotection of Benzoyl Group. Benzoylated compounds **7a**−**e**, **10a**−**e**, and **13a**−**e**, respectively, were stirred in methanolic ammonia (7 N, 100 equiv) at room temperature during 14 h. The solvent was removed under reduced pressure, and the crude residue was purified, using flash chromatography with elution gradient of AcOEt/MeOH to yield the desired compounds as amorphous solid. Following

this general procedure, analogues **8a**−**e**, **11a**−**e**, and **14a**−**e** were prepared and characterized as follows.

***N*^{1}-[(*E*)-4-Dimethoxyphosphonylbut-2-enyl]-uracil (8a).** Yield: 89%. ^{1}H NMR (400 MHz, $CDCl_3$): δ 9.55 (s, 1H), 7.13 (d, J = 8.0 Hz, 1H), 5.68−5.62 (m, 3H), 4.28 (m, 2H), 3.68 (d, J = 11.0 Hz, 6H), 2.65 (m, 2H). ^{31}P NMR (162 MHz, $CDCl_3$): δ 29.28.

***N*^{1}-[(*E*)-4-Dimethoxyphosphonylbut-2-enyl]-5-fluorouracil (8b).** Yield: 92%. HRMS (ESI): m/z calcd for $C_{10}H_{14}N_2FNaO_5P$ $[M+H]^+$ 315.0522, found 315.0540. ^{1}H NMR (400 MHz, $CDCl_3$): δ 9.55 (s, 1H), 7.28 (d, J = 5.6 Hz, 1H), 5.81−5.64 (m, 2H), 4.31 (m, 2H), 3.75 (d, J = 10.8 Hz, 6H), 2.65 (dd, J = 6.8, 22.0 Hz, 2H). ^{31}P NMR (162 MHz, $CDCl_3$): δ 28.53.

***N*^{1}-[(*E*)-4-Dimethoxyphosphonylbut-2-enyl]-5-chlorouracil (8c).** Yield: 90%. ^{1}H NMR (400 MHz, $CDCl_3$): δ 9.80 (s, 1H), 7.42 (d, 1H), 5.83−5.64 (m, 2H), 4.31 (m, 2H), 3.75 (d, J = 10.8 Hz, 6H), 2.66 (dd, J = 7.2, 22.0 Hz, 2H). ^{31}P NMR (162 MHz, $CDCl_3$): δ 28.55.

***N*^{1}-[(*E*)-4-Dimethoxyphosphonylbut-2-enyl]-5-bromouracil (8d).** Yield: 94%. HRMS (ESI): m/z calcd for $C_{10}H_{15}N_2O_5PBr$ $[M+H]^+$ 352.9902, found 352.9894. ^{1}H NMR (400 MHz, $CDCl_3$): δ 8.96 (s, 1H), 7.52 (s, 1H), 5.83−5.65 (m, 2H), 4.35 (dd, J = 4.4, 5.6 Hz, 2H), 3.77 (d, J = 10.8 Hz, 6H), 2.59 (dd, J = 7.2, 22.0 Hz, 2H). ^{31}P NMR (162 MHz, $CDCl_3$): δ 28.37.

***N*^{1}-[(*E*)-4-Dimethoxyphosphonyl-but-2-enyl]-thymine (8e).** Yield: 95%. HRMS (ESI): m/z calcd for $C_{11}H_{18}N_2O_5P$ $[M+H]^+$ 289.0953, found 289.0942. ^{1}H NMR (400 MHz, $CDCl_3$): δ 10.03 (s, 1H), 7.04 (d, J = 4.9 Hz, 1H), 5.71−5.73 (m, 2H), 4.50 (t, J = 4.8 Hz, 2H), 4.09 (d, J = 10.3 Hz, 6H), 2.59 (dd, J = 6.0, 22.2 Hz, 2H), 1.90 (s, 3H). ^{31}P NMR (162 MHz, $CDCl_3$): δ 29.55.

***N*^{1}-[(*Z*)-4-Dimethoxyphosphonylbut-2-enyl]-uracil (11a).** Yield: 92%. ^{1}H NMR (400 MHz, $CDCl_3$): δ 8.63 (s, 1H), 7.45 (d, J = 8.0 Hz, 1H), 5.65−5.75 (m, 3H), 4.44 (dd, J = 4.0, 6.4 Hz, 2H), 3.76 (d, J = 11.2 Hz, 6H), 2.65 (dd, J = 7.2, 22.4 Hz, 2H). ^{31}P NMR (162 MHz, $CDCl_3$): δ 28.53.

***N*^{1}-[(*Z*)-4-Dimethoxyphosphonylbut-2-enyl]-5-fluorouracil (11b).** Yield: 89%. HRMS (ESI): m/z calcd for $C_{10}H_{14}N_2FO_6P$ $[M+H]^+$ 293.0713, found 293.0703. ^{1}H NMR (400 MHz, $CDCl_3$): δ 9.78 (s, 1H), 7.65 (d, J = 6.0 Hz,1H), 5.79−5.62 (m, 2H), 4.43 (m, 2H), 3.78 (d, J = 10.8 Hz, 6H), 2.74 (dd, J = 8.0, 22.8 Hz, 2H). ^{31}P NMR (162 MHz, $CDCl_3$): δ 28.43.

***N*^{1}-[(*Z*)-4-Dimethoxyphosphonylbut-2-enyl]-5-chlorouracil (11c).** Yield: 90%. ^{1}H NMR (400 MHz, $CDCl_3$): δ 8.67 (s, 1H), 7.67 (s, 1H), 5.83−5.63 (m, 2H), 4.46 (dd, J = 3.6, 6.4 Hz, 2H), 3.78 (d, J = 12.0 Hz, 6H), 2.75 (dd, J = 8.0, 22.8 Hz, 2H). ^{31}P NMR (162 MHz, $CDCl_3$): δ 28.22.

***N*^{1}-[(*Z*)-4-Dimethoxyphosphonyl-but-2-enyl]-5-bromouracil (11d).** HRMS (ESI): m/z calcd for $C_{10}H_{15}N_2O_5PBr$ $[M+H]^+$ 352.9902, found 352.9891. ^{1}H NMR (400 MHz, CD_3OD): δ 8.03 (s, 1H), 5.69−5.84 (m, 2H), 4.45 (dd, J = 3.0, 5.3 Hz, 2H), 3.77 (d, J = 10.9 Hz, 6H), 2.59 (dd, J = 6.8, 23.0 Hz, 2H). ^{31}P NMR (162 MHz, CD_3OD): δ 30.36.

***N*^{1}-[(*Z*)-4-Dimethoxyphosphonyl-but-2-enyl]-thymine (11e).** Yield: 95%. HRMS (ESI): m/z calcd for $C_{11}H_{18}N_2O_5P$ $[M+H]^+$ 289.0953, found 289.0939. ^{1}H NMR (400 MHz, CD_3OD): δ 7.44 (d, J = 0.8 Hz, 1H), 5.64−5.76 (m, 2H), 4.42 (m, 2H), 3.77 (d, J = 10.8 Hz, 6H), 2.93 (dd, J = 7.2, 22.8 Hz, 2H), 1.90 (d, J = 0.8 Hz, 3H). ^{31}P NMR (162 MHz, CD_3OD): δ 34.46.

***N*^{1}-[(*E*)-5-Diethoxyphosphonyl-pent-2-enyl]-uracil (14a).** Yield: 93%. HRMS (ESI): m/z calcd for $C_{13}H_{21}N_2O_5NaP$ $[M+Na]^+$ 339.1086, found 339.1070. ^{1}H NMR (250 MHz, $CDCl_3$): δ 9.30 (br s, 1H), 7.53 (d, J = 8.0 Hz, 1H), 5.80 (dt, J = 6.4, 15.6 Hz, 1H), 5.63 (d, J = 8.0 Hz, 1H), 5.61 (dt, J = 6.0, 15.6 Hz, 1H′), 4.29 (d, J = 6.4 Hz, 2H), 2.58−2.30 (m, 2H), 1.89−1.75 (m, 2H). ^{31}P NMR (162 MHz, $CDCl_3$): δ 30.74.

***N*^{1}-[(*E*)-5-Diethoxyphosphonyl-pent-2-enyl]-5-fluorouracil (14b).** Yield: 86%. HRMS (ESI): m/z calcd for $C_{13}H_{20}FN_2O_5NaP$ $[M+Na]^+$ 357.0992, found 357.1009. ^{1}H NMR (250 MHz, $CDCl_3$): δ 10.33 (br s, 1H), 7.32 (d, J = 5.6 Hz, 1H), 5.82 (dt, J = 6.6, 15.2 Hz, 1H), 5.52 (dt, J = 6.8, 15.2 Hz, 1H), 4.27 (d, J = 6.8 Hz, 2H), 4.03−4.17 (m, 4H), 2.31−2.62 (m, 2H), 1.78−1.90 (m, 2H), 1.30 (t, J = 7.2 Hz, 6H). ^{31}P NMR (162 MHz, $CDCl_3$): δ 30.83.

***N*^{1}-[(*E*)-5-Diethoxyphosphonyl-pent-2-enyl]-5-chlorouracil (14c).** Yield: 86%. HRMS (ESI): m/z calcd for $C_{13}H_{20}ClN_2O_5NaP$ $[M+Na]^+$ 373.0696, found 373.0690. ^{1}H NMR (250 MHz, $CDCl_3$): δ 7.41 (s, 1H), 5.80 (dt, J = 6.4, 15.2 Hz, 1H), 5.53 (dt, J = 6.8, 15.2 Hz, 1H), 4.27 (d, J = 6.4 Hz, 2H), 4.40−4.16 (m, 4H), 2.30−2.69 (m, 2H), 1.75−1.99 (m, 2H), 1.28 (t, J = 7.2 Hz, 6H). ^{31}P NMR (162 MHz, $CDCl_3$): δ 30.66.

***N*^{1}-[(*E*)-5-Diethoxyphosphonyl-pent-2-enyl]-5-bromouracil (14d).** Yield: 76%. HRMS (ESI): m/z calcd for $C_{13}H_{20}BrN_2O_5NaP$ $[M+Na]^+$) 417.0191, found 417.0181. ^{1}H NMR (250 MHz, $CDCl_3$): δ 8.69 (br s, 1H), 7.54 (s, 1H), 5.85 (dt, J = 6.4, 15.2 Hz, 1H), 5.55 (dt, J = 6.4, 15.2 Hz, 1H), 4.31 (d, J = 6.4 Hz, 2H), 4.12−4.04 (m, 4H), 2.45−2.37 (m, 2H), 1.88−1.80 (m, 2H), 1.32 (t, J = 7.0 Hz, 6H). ^{31}P NMR (162 MHz, $CDCl_3$): δ 30.49.

***N*^{1}-[(*E*)-5-Diethoxyphosphonyl-pent-2-enyl]-thymine (14e).** Yield: 87%. HRMS (ESI): m/z calcd for $C_{14}H_{23}N_2O_5NaP$ $[M+Na]^+$ 353.1242, found 353.1231. ^{1}H NMR (250 MHz, $CDCl_3$): δ 9.90 (br s, 1H), 7.00 (s, 1H), 5.72 (dt, J = 6.3, 15.5 Hz, 1H), 5.51 (dt, J = 6.3, 15.5 Hz, 1H), 4.25 (d, J = 6.3 Hz, 2H), 4.19−4.00 (m, 4H), 2.63−2.31 (m, 2H), 1.94−1.72 (m, 2H), 1.88 (s, 3H), 1.29 (t, J = 7.0 Hz, 6H). ^{31}P NMR (162 MHz, $CDCl_3$): δ 30.81.

General Procedure for the Deprotection of Phosphonate Diesters. To a CH_2Cl_2 (5 mL) solution of phosphonate diester, TMSBr (6 equiv) was added and stirred at room temperature until starting material disappeared on TLC. MeOH (5 mL) was added and evaporated with heating (ca. 60 °C). MeOH (5 mL) was added again, and this procedure was repeated three times. The residue was extracted with ultrapure H_2O and CH_2Cl_2, and the inorganic phase was evaporated to yield the expected compound as an amorphous solid. Following this general procedure, analogues **6a**−**e**, **9a**−**e**, **12a**−**e**, **15a**−**e** were prepared and characterized as follows.

***N*^{1}-[(*E*)-3-Dihydroxyphosphonyl-prop-2-enyl]-5-fluoro-uracil (6b).** Yield: 94%. HRMS (ESI): m/z calcd for $C_7H_9FN_2O_5P$ $[M+H]^+$ 251.0233, found 251.0251. ^{1}H NMR (400 MHz, CD_3OD): δ 7.82 (d, J = 6.0 Hz, 1H), 6.64 (ddt, J = 4.8, 17.6, 22.0 Hz, 1H), 5.94 (t, J = 17.6 Hz, 1H), 4.49 (m, 2H). ^{31}P NMR (161.9 MHz, CD_3OD): δ 13.82. Purity >99%. HPLC t_R = 2 min 15 s; acetonitrile/H_2O (5:95).

***N*^{1}-[(*E*)-3-Dihydroxyphosphonyl-prop-2-enyl]-thymine (6e).** Yield: 85%. HRMS (ESI): m/z calcd for $C_8H_{12}N_2O_5P$ $[M+H]^+$ 247.0484, found 247.0475. ^{1}H NMR (400 MHz, CD_3OD): δ 7.39 (s, 1H), 6.73 (ddt, J = 4.5, 17.5, 22.0 Hz, 1H), 5.85 (t, J = 17.5 Hz, 1H), 4.49 (m, 2H), 1.87 (s, 3H). ^{31}P NMR (161.9 MHz, CD_3OD): δ 13.99. Purity >97%. HPLC t_R = 2 min 8 s; acetonitrile/H_2O (5:95).

***N*^{1}-[(*E*)-4-Dihydroxyphosphonyl-but-2-enyl]-5-fluorouracil (9b).** Yield: 95%. HRMS (ESI): m/z calcd for $C_8H_{10}N_2O_5NaPF$ $[M+Na]^+$ 287.0209, found 287.0197. ^{1}H NMR (250 MHz, CD_3OD): δ 7.77 (d, J = 6.3 Hz, 1H), 5.67−5.86 (m, 2H), 4.32 (m, 2H), 2.63 (dd, J = 6.0, 21.5 Hz, 2H′). ^{31}P NMR (161.9 MHz, CD_3OD): δ 24.15. Purity >98%. HPLC t_R = 2 min 7 s; acetonitrile/H_2O (5:95).

***N*^{1}-[(*E*)-4-Dihydroxyphosphonyl-but-2-enyl]-thymine (9e).** Yield: 87%. HRMS (ESI): m/z calcd for $C_9H_{14}N_2O_5P$ $[M+H]^+$ 261.0640, found 261.0639. ^{1}H NMR (400 MHz, CD_3OD): δ 7.28 (s, 1H), 5.57−5.70 (m, 2H), 4.30 (m, 2H), 2.49 (m, 2H), 1.77 (s, 3H). ^{31}P NMR (161.9 MHz, CD_3OD): δ 23.58. Purity >99%. HPLC t_R = 2 min 10 s; acetonitrile/H_2O (10:90).

***N*^{1}-[(*Z*)-4-Dihydroxyphosphonyl-but-2-enyl]-5-fluorouracil (12b).** Yield: 96%. HRMS (ESI): m/z calcd for $C_8H_{10}N_2O_5NaPF$ $[M+Na]^+$ 287.0209, found 287.0204. ^{1}H NMR (250 MHz, CD_3OD): δ 7.85 (d, J = 6.3 Hz, 1H), 5.62−5.85 (m, 2H), 4.42 (dd, J = 3.4, 6.7 Hz, 2H), 2.78 (dd, J = 7.3, 22.0 Hz, 2H). ^{31}P NMR (161.9 MHz, CD_3OD): δ 24.16. Purity >99%. HPLC t_R = 2 min; acetonitrile/H_2O (5:95, v/v).

***N*^{1}-[(*Z*)-4-Dihydroxyphosphonyl-but-2-enyl]-5-bromouracil (12d).** HRMS (ESI): m/z calcd for $C_8H_{11}N_2O_5PBr$ $[M+H]^+$ 324.9589, found 324.9585. ^{1}H NMR (400 MHz, CD_3OD): δ 8.05 (s, 1H),

5.65−5.75 (m, 2H), 4.47 (dd, J = 3.2, 6.0 Hz, 2), 2.76 (dd, J = 8.0, 22.4 Hz, 2H). ^{31}P NMR (162 MHz, CD_3OD): δ 23.66. Purity >98%. HPLC t_R = 2 min 4 s; acetonitrile/H_2O (5:95).

***N*^{1}-[(*Z*)-4-Dihydroxyphosphonyl-but-2-enyl]-thymine (12e).** Yield: 89%. HRMS (ESI): m/z calcd for $C_9H_{14}N_2O_5P$ $[M+H]^+$ 261.0632, found 261.0639. ^{1}H NMR (400 MHz, CD_3OD): δ 7.46 (d, J = 1.2 Hz, 1H), 5.61−5.80 (m, 2H), 4.43 (m, 2H), 2.49 (m, 2H), 1.86 (d, J = 1.2 Hz, 3H). ^{31}P NMR (161.9 MHz, CD_3OD): δ 23.71. Purity >99%. HPLC t_R = 2 min 20 s; acetonitrile/H_2O (5:95).

***N*^{1}-[(*E*)-5-Dihydroxyphosphonyl-pent-2-enyl]-uracil (15a).** Yield: 78%. HRMS (ESI): m/z calcd for $C_9H_{12}N_2O_5P$ $[M-H]^-$ 259.0484, found 259.0496. ^{1}H NMR (400 MHz, CD_3OD): δ 7.53 (d, J = 8.0 Hz, 1H), 5.80 (dt, J = 6.4, 15.6 Hz, 1H), 5.63 (d, J = 8.0 Hz, 1H), 5.61 (dt, J = 6.0, 15.6 Hz, 1H), 4.29 (d, J = 6.4 Hz, 2H), 2.58−2.30 (m, 2H), 1.89−1.75 (m, 2H). ^{31}P NMR (161.9 MHz, CD_3OD): δ 30.17. Purity >98%. HPLC t_R = 2 min 20 s; acetonitrile/H_2O (5:95).

***N*^{1}-[(*E*)-5-Dihydroxyphosphonyl-pent-2-enyl]-5-fluorouracil (15b).** Yield: 90%. HRMS (ESI): m/z calcd for $C_9H_{13}FN_2O_5P$ $[M+H]^+$ 279.0546, found 279.0550. ^{1}H NMR (400 MHz, CD_3OD): δ 7.78 (d, J = 6.4 Hz, 1H), 5.86 (dt, J = 6.8, 15.2 Hz, 1H), 5.61 (dt, J = 6.4, 15.2 Hz, 1H), 4.30 (d, J = 6.4 Hz, 2H), 2.31−2.62 (m, 2H), 1.78−1.91 (m, 2H). ^{31}P NMR (161.9 MHz, CD_3OD): δ 29.65. Purity >99%. HPLC t_R = 2 min 16 s; acetonitrile/H_2O (5:95).

***N*^{1}-[(*E*)-5-Dihydroxyphosphonyl-pent-2-enyl]-5-chlorouracil (15c).** Yield: 85%. HRMS (ESI): m/z calcd for $C_9H_{13}N_2ClO_5P$ $[M+H]^+$ 295.0251, found 295.0248. ^{1}H NMR (400 MHz, CD_3OD): δ 7.88 (s, 1H) 5.86 (dt, J = 6.4, 15.2 Hz, 1H), 2.32−2.62 (m, 2H), 5.62 (dt, J = 6.0, 15.6 Hz, 1H), 4.32 (d, J = 6.0 Hz, 2H), 1.75−1.88 (m, 2H). ^{31}P NMR (161.9 MHz, CD_3OD): δ 29.32. Purity >95%. HPLC t_R = 2 min 34 s; acetonitrile/H_2O (5:95).

***N*^{1}-[(*E*)-5-Dihydroxyphosphonyl-pent-2-enyl]-5-bromouracil (15d).** Yield: 84%. HRMS (ESI): m/z calcd for $C_9H_{11}BrN_2O_5P$ $[M-H]^-$ 336.9589, found 336.9577. ^{1}H NMR (400 MHz, CD_3OD): δ 7.97 (s, 1H), 5.86 (dt, J = 6.6, 15.2 Hz, 1H), 5.63 (dt, J = 6.4, 15.2 Hz, 1H), 4.29 (d, J = 6.0 Hz, 2H), 2.62−2.32 (m, 2H), 1.89−1.78 (m, 2H). ^{31}P NMR (161.9 MHz, CD_3OD): δ 29.31. Purity >98%. HPLC t_R = 2 min 29 s; acetonitrile/H_2O (5:95).

***N*^{1}-[(*E*)-5-Dihydroxyphosphonyl-pent-2-enyl]-thymine (15e).** Yield: 90%. HRMS (ESI): m/z calcd for $C_{10}H_{14}N_2O_5P$ $[M-H]^-$ 273.0640, found 273.0633. ^{1}H NMR (400 MHz, CD_3OD): δ 7.41 (d, J = 0.8 Hz, 1H), 5.80 (dt, J = 6.3, 15.4 Hz, 1H), 5.61 (dt, J = 6.0, 15.4 Hz, 1H), 4.29 (d, J = 6.0 Hz, 2H), 2.63−2.30 (m, 2H), 1.90−1.80 (m, 2H), 1.88 (s, 3H). ^{31}P NMR (161.9 MHz, CD_3OD): δ 29.41. Purity >98%. HPLC t_R = 2 min 27 s; acetonitrile/H_2O (5:95).

General Procedure for the Synthesis of Bis(Pom)-allylphosphonates. To a ACN (18 mL) solution of C5-substituted dimethyl allylphosphonate (**8d**,**e** and **11d**,**e**) (2.6 g, 17.3 mmo1) and anhydrous sodium iodide (5.2 g, 34.6 mmol), chloromethyl pivalate (6.58 g, 43.3 mmol) was added. This solution was stirred at reflux for 48 h under positive pressure of dry Ar. After cooling, 170 mL of diethyl ether was added to this mixture and washed by 35 mL of water. The organic layer was dried on magnesium sulfate, evaporated, and purified by chromatography on silica gel (EtOAc/EP 1:4) to give pure Bis-(POM) allylphosphonate as slightly yellow oil. Following this general procedure, analogues **16**−**19** were prepared and characterized as follows.

***N*^{1}-[(*E*)-4-Bis(pivaloyloxymethyl)phosphinyl-buten-2-yl]-thymine (16).** Yield: 47%. HRMS (ESI): m/z calcd for $C_{21}H_{33}N_2O_9NaP$ $[M+Na]^+$ 511.1821, found 511.1837. ^{1}H NMR (400 MHz, CD_3OD): δ 7.37 (d, J = 0.9 Hz, 1H), 5.85−5.74 (ddt, J = 5.1, 15.6 Hz, 1H), 5.66 (m, 5H), 4.32 (t, J = 5.2 Hz, 2H), 2.82 (dd, J = 7.2, 22.5, Hz, 2H), 1.87 (s, 3H) 1.23 (s, 18H). ^{31}P NMR (161.9 MHz, CD_3OD): δ 27.3. Purity >96%. HPLC t_R = 5 min 12 s; acetonitrile/H_2O (60:40).

***N*^{1}-[(*Z*)-4-Bis(pivaloyloxymethyl)phosphinyl-2-butenyl]-thymine (17).** Yield: 46%. HRMS (ESI): m/z calcd for $C_{21}H_{33}N_2O_9NaP$ $[M+Na]^+$ 511.1821, found 511.1828. ^{1}H NMR (400 MHz, CD_3OD): δ 7.46 (d, J = 1.2 Hz, 1H), 5.78−5.60 (m, 7H), 4.40 (dd, J = 3.8, 5.5 Hz, 2H), 3.01 (dd, J = 7.8, 23.2 Hz, 2H), 1.88 (d, J = 1.1 Hz, 3H), 1.24 (d, J = 3.2 Hz, 18H). ^{31}P NMR (162 MHz, CD_3OD): δ 27.6. Purity >96%. HPLC t_R = 5 min 44 s; acetonitrile/H_2O (60:40).

***N*^{1}-[(*E*)-4-Bis(pivaloyloxymethyl)phosphinyl-2-butenyl]-5-bromouracil (18).** Yield: 78%. HRMS (ESI): m/z calcd for $C_{20}H_{30}N_2O_9NaPBr$ $[M+Na]^+$ 575.0770, found 575.0764. ^{1}H NMR (400 MHz, CD_3OD): δ 7.98 (s, 1H), 5.85−5.76 (m, 1H), 5.75−5.62 (m, 5H), 4.36 (t, J = 5.1 Hz, 2H), 2.82 (dd, J = 6.9, 22.5 Hz, 2H), 1.23 (s, 18H). ^{31}P NMR (162 MHz, CD_3OD): δ 27.1. Purity >96%. HPLC t_R = 6 min 13 s; acetonitrile/H_2O (60:40).

***N*^{1}-[(*Z*)-4-Bis(pivaloyloxymethyl)phosphinyl-2-butenyl]-5-bromouracil (19).** HRMS (ESI): m/z calcd for $C_{20}H_{30}N_2O_9NaPBr$ $[M+Na]^+$ 575.0770, found 575.0778. ^{1}H NMR (400 MHz, CD_3OD): δ 8.06 (s, 1H), 5.70−5.52 (m, 6H), 4.45 (dd, J = 3.7, 6.8 Hz, 2H), 3.01 (dd, J = 23.4, 7.8 Hz, 2H), 1.24 (s, 18H). ^{31}P NMR (100 MHz, CD_3OD) δ 27.5. Purity >95%. HPLC t_R = 7 min 1 s; acetonitrile/H_2O (60:40).

Protein Purification and Enzymatic Assays. The recombinant hTMPK and hUCK were prepared as described.[19,27] The activities of hTMPK and hUCK were followed by the coupled spectrophotometric assay.[17,19] Assays were carried out at 37 °C in a Tris-HCl 50 mM pH = 7.4 buffer containing 50 mM KCl, 5 mM $MgCl_2$, 1 mM ATP, 0.2 mM NADH, 1 mM phosphoenolpyruvate, 1 mM DTT, 4 U.μL^{-1} pyruvate kinase, and 4 U.μL^{-1} lactate dehydrogenase (total volume: 130 μL). The reaction was started by adding the (d)NMP or (d)NMP analogue, and the decrease in absorbance at 340 nm was measured. The kinase concentrations were 4 nM to 8 μM in order to measure initial rates below 0.2 ΔA/min. For inhibition studies, the inhibitor was added after the enzyme, and then the reaction was started. All experiments were done at least twice.

Thymidine kinase assays were done as described[28] at 37 °C during 15 min, in the presence of 5 mM ATP and 1 μM [^{3}H]-T in a Tris-HCl 50 mM pH = 7.6 buffer containing 2 mM $MgCl_2$, 0.5 mg/mL bovine serum albumin, and 5 mM DTT. The assays were done in triplicate. The addition of 0.3 mM 5-Cl-UbutP (**9d**) decreased TK1 (4 ng)[28] and TK2 (1 ng)[29] activity by 11% and 13%, respectively (standard deviations 1% and 2.6%).

Crystal Structure Determination. The hTMPK was equilibrated by dialysis against 50 mM Tris-HCl pH 8.0 buffer containing 200 mM KCl, 0.5 mM DTT. The crystal screening was done on a Cartesian robot using Quiagen screens in 96 well vapor diffusion plates (Greiner). Final crystals were grown at 20 °C mixing 1 μL of 20 mg/mL hTMPK, 8 mM (*E*)-TbutP (**9e**), 10 mM ATP, 5 mM $MgCl_2$, and 1 μL of 14% (w/v) PEG 3350, 0.1 M Hepes pH 7.5. Crystals were soaked in the reservoir solution supplemented with glycerol to a final concentration of 20% (w/v) and frozen at 100 K in liquid nitrogen. Data were collected on the beamline PROXIMA-1 of SOLEIL synchrotron (Gif-sur-Yvette, France) at a wavelength of 0.98 Å.

The data reduction and scaling were done using *XDS* package.[30] The structure was solved by molecular replacement using Phaser[31] and the pdb entry 1e2g as the search model. The space group is *C*2 with one molecule per asymmetric unit. The structure was rebuilt using Coot and refined with Phenix.[32,33] Statistics for data reduction and structure refinement are presented in Supporting Information Table 1. The structure of human TMP kinase in complex with (*E*)-TbutP (**9e**) is being deposited in the Protein Data Bank.

Antiviral Assays. The herpes and vaccinia virus assays were based on inhibition of virus-induced cytopathicity in HEL cells [herpes simplex virus type 1 (HSV-1) (KOS), HSV-2 (G), HSV-1 TK$^-$ (KOS acyclovir resistant, ACV^r) and vaccinia virus (VV)]. Confluent cell cultures in microtiter 96-well plates were inoculated with 100 $CCID_{50}$ of virus (1 $CCID_{50}$ being the virus dose to infect 50% of the cell cultures). After a 1 h virus adsorption period, residual virus was removed, and the cell cultures were

incubated in the presence of varying concentrations (200, 40, 8 μM) of the tested compounds. Viral cytopathicity was recorded as soon as it reached completion in the control virus-infected cell cultures that were not treated with the test compounds.

Confluent human embryonic lung (HEL) fibroblasts were grown in 96-well microtiter plates and infected with the human cytomegalovirus (HCMV) strains Davis and AD-169 at 100 PFU per well. After a 2 h incubation period, residual virus was removed and the infected cells were further incubated with medium containing different concentrations of the test compounds (in duplicate). After incubation for 7 days at 37 °C, virus-induced cytopathogenicity was monitored microscopically after ethanol fixation and staining with Giemsa. Antiviral activity was expressed as the EC_{50} or compound concentration required to reduce virus-induced cytopathogenicity by 50%. EC_{50} values were calculated from graphic plots of the percentage of cytopathogenicity as a function of concentration of the compounds.

The laboratory wild-type VZV strain OKA and the thymidine kinase-deficient VZV strain 07/1 were used. Confluent HEL cells grown in 96 well microtiter plates were inoculated with VZV at an input of 20 PFU per well. After a 2 h incubation period, residual virus was removed and varying concentrations of the test compounds were added (in duplicate). Antiviral activity was expressed as the 50% effective concentration required to reduce viral plaque formation after 5 days by 50% as compared with untreated controls.

Cytotoxicity Assays. Cytotoxicity measurements were based on the inhibition of HEL cell growth. HEL cells were seeded at a rate of 5×10^3 cells/well into 96 well microtiter plates and allowed to proliferate for 24 h. Then, medium containing different concentrations of the test compounds was added. After 3 days of incubation at 37 °C, the cell number was determined with a Coulter counter. The 50% cytostatic concentration (CC_{50}) was calculated as the compound concentration required reducing cell growth by 50% relative to the number of cells in the untreated controls. CC_{50} values were estimated from graphic plots of the number of cells (percentage of control) as a function of the concentration of the test compounds. Cytotoxicity was also expressed as the minimum cytotoxic concentration (MCC) or the compound concentration that causes a microscopically detectable alteration of cell morphology.

Acknowledgment. These studies were supported by Université Pierre et Marie Curie (UPMC) the Centre National de Recherche Scientifique (Unité Mixte de Recherche 6005, Formation de Recherche en Evolution 2852 and Unité Propre de Recherche 3082), the Agence Nationale de Recherche (grant ANR-05-BLAN-0368-02), the Concerted Actions (GOA 05/19) of the K. U. Leuven and the Fondation pour la Recherche Médicale (P. Meyer and C. Caillat). We thank Michèle Reboud (UPMC) for laboratory facilities, Sylvie Pochet and Laurence Dugué (Institut Pasteur, France) for synthesizing the MABA derivatives, and Leentje Persoons, Lies Van den Heurck, Anita Camps, and Steven Carmans (Rega Institute, Leuven, Belgium) for expert assistance in cellular assays.

Supporting Information Available: Structural data from X-ray of human thymidilate kinase (SI-Table 1). Circular dichroism spectroscopic data obtained with hUCK and some selected ANPs compared to natural substrates (SI-Table 2). Inhibition of human UCK by [*E*]-5Cl-UbutP (**9c**) (SI-Figure 1). This material is available free of charge via the Internet at http://pubs.acs.org.

References

(1) De Clercq, E. Acyclic nucleoside phosphonates: past, present and future. Bridging chemistry to HIV, HBV, HCV, HPV, adeno-, herpes-, and poxvirus infections: the phosphonate bridge. *Biochem. Pharmacol.* **2007**, *73*, 911–922.
(2) Balzarini, J.; Pannecouque, C.; De Clercq, E.; Aquaro, S.; Perno, C. F.; Egberink, H.; Holy, A. Antiretrovirus activity of a novel class of acyclic pyrimidine nucleoside phosphonates. *Antimicrob. Agents Chemother.* **2002**, *46*, 2185–2193.
(3) Votruba, I.; Bernaerts, R.; Sakuma, T.; De Clercq, E.; Merta, A.; Rosenberg, I.; Holy, A. Intracellular phosphorylation of broad-spectrum anti-DNA virus agent (S)-9-(3-hydroxy-2-phosphonylmethoxypropyl)adenine and inhibition of viral DNA synthesis. *Mol. Pharmacol.* **1987**, *32*, 524–529.
(4) Cihlar, T.; Chen, M. S. Identification of enzymes catalyzing two-step phosphorylation of cidofovir and the effect of cytomegalovirus infection on their activities in host cells. *Mol. Pharmacol.* **1996**, *50*, 1502–1510.
(5) Robbins, B. L.; Greenhaw, J.; Connelly, M. C.; Fridland, A. Metabolic pathways for activation of the antiviral agent 9-(2-phosphonylmethoxyethyl)adenine in human lymphoid cells. *Antimicrob. Agents Chemother.* **1995**, *39*, 2304–2308.
(6) Koch, K.; Chen, Y.; Feng, J. Y.; Borroto-Esoda, K.; Deville-Bonne, D.; Gallois-Montbrun, S.; Janin, J.; Morera, S. *Nucleosides Nucleotides Nucleic Acids* **2009**, *28*, 776–792.
(7) Tuske, S.; Sarafianos, S. G.; Clark, A. D., Jr.; Ding, J.; Naeger, L. K.; White, K. L.; Miller, M. D.; Gibbs, C. S.; Boyer, P. L.; Clark, P.; Wang, G.; Gaffney, B. L.; Jones, R. A.; Jerina, D. M.; Hughes, S. H.; Arnold, E. Structures of HIV-1 RT-DNA complexes before and after incorporation of the anti-AIDS drug tenofovir. *Nat. Struct. Mol. Biol.* **2004**, *11*, 469–474.
(8) Magee, W. C.; Hostetler, K. Y.; Evans, D. H. Mechanism of inhibition of vaccinia virus DNA polymerase by cidofovir diphosphate. *Antimicrob. Agents Chemother.* **2005**, *49*, 3153–3162.
(9) Magee, W. C.; Aldern, K. A.; Hostetler, K. Y.; Evans, D. H. Cidofovir and (S)-9-[3-hydroxy-(2-phosphonomethoxy)propyl]-adenine are highly effective inhibitors of vaccinia virus DNA polymerase when incorporated into the template strand. *Antimicrob. Agents Chemother.* **2008**, *52*, 586–597.
(10) Topalis, D.; Alvarez, K.; Barral, K.; Munier-Lehmann, H.; Schneider, B.; Véron, M.; Guerreiro, C.; Mulard, L.; El-Amri, C.; Canard, B.; Deville-Bonne, D. Acyclic phosphonate nucleotides and human adenylate kinases: impact of a borano group on alpha-P position. *Nucleosides Nucleotides Nucleic Acids* **2008**, *27*, 319–331.
(11) Topalis, D.; Kumamoto, H.; Amaya Velasco, M. F.; Dugue, L.; Haouz, A.; Alexandre, J. A.; Gallois-Montbrun, S.; Alzari, P. M.; Pochet, S.; Agrofoglio, L. A.; Deville-Bonne, D. Nucleotide binding to human UMP-CMP kinase using fluorescent derivatives a screening based on affinity for the UMP-CMP binding site. *FEBS J.* **2007**, *274*, 3704–3714.
(12) Topalis, D.; Broggi, J.; Alexandre, J. A.; Pradere, U.; Roy, V.; Berteina-Raboin, S.; Agrofoglio, L. A.; Deville-Bonne, D. Evaluation of C-5 Substituted uracil acyclic phosphonates as substrates or inhibitors for dTMP and UMP−CMP kinases and potential anti-pox derivatives. *Antivir. Res.* **2008**, *78*, A65.
(13) Kumamoto, H.; Broggi, J.; Topalis, D.; Pradere, U.; Roy, V.; Berteina-Raboin, S.; Nolan, S. P.; Deville-Bonne, D.; Snoeck, R.; Garin, D.; Agrofoglio, L. Preparation of acyclo nucleoside phosphonate analogues based-on cross-metathesis. *Tetrahedron* **2008**, *64*, 3517–3526.
(14) Chatterjee, A. K.; Choi, T.-L.; Sanders, D. P.; Grubbs, R. H. A general model for selectivity in olefin cross metathesis. *J. Am. Chem. Soc.* **2003**, *125*, 11360–11370.
(15) Cruickshank, K. A.; Jiricny, J.; Reese, C. B. The benzoylation of uracil and thymine. *Tetrahedron Lett.* **1984**, *25*, 681–684.
(16) Vepsalainen, J. J. Bisphosphonate prodrugs: a new synthetic strategy to tetraacyloxymethyl esters of methylenebisphosphonates. *Tetrahedron Lett.* **1999**, *40*, 8491–8493.
(17) Alexandre, J. A.; Roy, B.; Topalis, D.; Pochet, S.; Perigaud, C.; Deville-Bonne, D. Enantioselectivity of human AMP, dTMP and UMP-CMP kinases. *Nucleic Acid Res.* **2007**, *35* (14), 4895–4904.
(18) Huang, S. H.; Tang, A.; Drisco, B.; Zhang, S. Q.; Seeger, R.; Li, C.; Jong, A. Human dTMP kinase: gene expression and enzymatic activity coinciding with cell cycle progression and cell growth. *DNA Cell Biol.* **1994**, *13*, 461–471.
(19) Pochet, S.; Dugué, L.; Labesse, G.; Delepierre, M.; Munier-Lehmann, H. Comparative study of purine and pyrimidine nucleoside analogues acting on the thymidylate kinases of *Mycobacterium tuberculosis* and of humans. *ChemBioChem* **2003**, *4*, 742–747.
(20) Ostermann, N.; Schlichting, I.; Brundiers, R.; Konrad, M.; Reinstein, J.; Veit, T.; Goody, R. S.; Lavie, A. Insights into the phosphoryltransfer mechanism of human thymidylate kinase gained from crystal structures of enzyme complexes along the reaction coordinate. *Structure* **2000**, *8*, 629–642.

(21) Deville-Bonne, D.; El-Amri, C.; Meyer, P.; Chen, Y.; Agrofoglio, L. A.; Janin, J. Human and viral nucleoside/nucleotide kinases involved in antiviral drug activation: Structural and catalytic properties. *Antivir. Res.* **2010**, *86*, 101–120.
(22) Chen, Y. L.; Lin, D. W.; Chang, Z. F. Identification of a putative human mitochondrial thymidine monophosphate kinase associated with monocytic/macrophage terminal differentiation. *Genes Cells* **2008**, *13*, 679–689.
(23) Hiratsuka, T. J. Affinity labeling of the myosin ATPase with ribose-modified fluorescent nucleotides and vanadate. *Biochemistry* **1984**, *96*, 147–154.
(24) Hernandez, A.-I.; Balzarini, J.; Karlsson, A.; Camarasa, M.-J.; Pérez-Pérez, M.-J. Acyclic nucleotide analogues as novel inhibitors of human mitochondrial thymidine kinase. *J. Med. Chem.* **2002**, *45*, 4254–4263.
(25) (a) Choo, H.; Beadle, J.; Chong, Y.; Trahan, J.; Hostetler, K. Synthesis of the 5-phosphono-pent-2-en-1-yl nucleosides: A new class of antiviral acyclic nucleoside phosphonates. *Bioorg. Med. Chem.* **2007**, *15*, 1771–1779. (b) Choo, H.; Beadle, J.; Kern, E.; Prichard, M.; KA., K.; Hartline, C.; Trahan, J.; Aldern, K.; Korba, B.; Hostetler, K. Antiviral activities of novel 5-phosphono-pent-2-en-1-yl nucleosides and their alkoxyalkyl phosphonoesters. *Antimicrob. Agents Chemother.* **2007**, *51*, 611–615.
(26) Topalis, D.; Collinet, B.; Gasse, C.; Dugue, L.; Balzarini, J.; Pochet, S.; Deville-Bonne, D. Substrate specificity of vaccinia virus thymidylate kinase. *FEBS J.* **2005**, *272*, 6254–6265.
(27) Pasti, C.; Gallois-Montbrun, S.; Munier-Lehmann, H.; Veron, M.; Gilles, A.-M.; Deville-Bonne, D. Reaction of human UMP-CMP kinase with natural and analog substrates. *Eur. J. Biochem.* **2003**, *270*, 1784–1790.
(28) Kosinska, U.; Carnrot, C.; Eriksson, S.; Wang, L.; Eklund, H. Structure of the substrate complex of thymidine kinase from Ureaplasma urealyticum and investigations of possible drug targets for the enzyme. *FEBS J.* **2005**, *272*, 6365–6372.
(29) Wang, L.; Munch-Petersen, B.; Herrstrom Sjoberg, A.; Hellman, U.; Bergman, T.; Jornvall, H.; Eriksson, S. Human thymidine kinase 2: molecular cloning and characterisation of the enzyme activity with antiviral and cytostatic nucleoside substrates. *FEBS Lett.* **1999**, *443*, 170–174.
(30) Kabsch, B. Automatic processing of rotation diffraction data from crystals of initially unknown symmetry and cell constants. *J. Appl. Crystallogr.* **1993**, *26*, 795–800.
(31) Storoni, L. C.; McCoy, A. J.; Read, R. J. Likelihood-enhanced fast rotation functions. *Acta Crystallogr., Sect. D* **2004**, *60*, 432–438.
(32) Emsley, P.; Cowtan, K. Coot: model-building tools for molecular graphics. *Acta Crystallogr., Sect. D* **2004**, *60*, 2126–2132.
(33) Adams, P. D.; Grosse-Kunstleve, R. W.; Hung, L.-W.; Ioerger, T. R.; McCoy, A. J.; Moriarty, N. W.; Read, R. J.; Sacchettini, J. C.; Sauter, N. K.; Terwilliger, T. C. PHENIX: building new software for automated crystallographic structure determination. *Acta Crystallogr., Sect. D* **2002**, *58*, 1948–1954.